Available online at www.sciencedirect.com
ScienceDirect
Ceramics International 37 (2011) 1133–1137
CERAMICS INTERNATIONAL
www.elsevier.com/locate/ceramint

Short communication

Preparation and characterization of transparent Tm:YAG ceramics

Wen-Xin Zhang [a,b], Yu-Bai Pan [a,*], Jun Zhou [a,b], Wen-Bin Liu [a], Jiang Li [a], Yu-Wan Zou [c], Zhi-Yi Wei [c]

[a] Key Laboratory of Transparent and Opto-functional Advanced Inorganic Materials, Shanghai Institute of Ceramics, Chinese Academy of Sciences, Shanghai 200050, PR China
[b] Graduate School of the Chinese Academy of Sciences, Beijing 100039, PR China
[c] Laboratory of Optical Physics, Institute of Physics, Chinese Academy of Sciences, Beijing 100190, PR China

Received 23 June 2010; received in revised form 11 October 2010; accepted 6 November 2010
Available online 3 December 2010

Abstract

Polycrystalline $(Y_{3-x}Tm_x)Al_5O_{12}$ ($x = 0$, 0.18, 0.9, 1.5, 3) ceramics were fabricated by a solid-state reaction method using high-purity micrometer-sized powders. Tm-doped ceramics with an almost perfect pore-free structure and high transparency were obtained by advanced ceramic processing. The average grain size and grain boundary width were 15 μm and 1 nm, respectively. The $Y_{2.82}Tm_{0.18}Al_5O_{12}$ (6 at.% Tm:YAG) ceramic slab (5 mm × 5 mm × 3.5 mm) was end-pumped by a Ti:sapphire laser at 785 nm and the maximum output power of 725 mW was obtained with a slope efficiency of 36.2% at 2012 nm.

Keywords: B. Microstructure; C. Optical properties; Transparent ceramic

1. Introduction

Thulium-doped YAG lasers are important sources in the eye-safe 2 μm spectral region and have extensive applications in remote sensing and in medical and military technologies. Thulium has several favorable properties with respect to laser-diode pumping, such as a strong absorption band at 785 nm, which overlaps the emission from AlGaAs laser diodes, and an efficient cross-relaxation process yielding two ions in the upper laser level for each absorbed pump photon. The rapid development of efficient high-power laser-diode arrays in the past decade has, therefore, increased the interest in laser materials doped or co-doped with thulium [1].

Since a high-efficiency polycrystalline Nd:YAG ceramic laser was reported by the present authors in 1995 [2], various transparent ceramic laser materials such as Yb:YSAG and Nd:Y_2O_3 have been developed [3–9]. Compared to the more commonly used single crystals, polycrystalline ceramics can be highly doped, cheaper, faster and easier to produce.

In this paper, highly transparent $(Y_{3-x}Tm_x)Al_5O_{12}$ ($x = 0$, 0.18, 0.9, 1.5, 3) ceramics were successfully fabricated. The appearances of the starting powders, the XRD patterns, and the in-line transmittance spectra of the Tm:YAG ceramics were investigated. Moreover, 6 at.% Tm:YAG ceramic was chosen to be used in the laser experiment. The maximum output power of 725 mW was obtained with a slope efficiency of 36.2% and optical-to-optical efficiency of 19.9% at 2012 nm.

2. Experimental procedure

2.1. Ceramic fabrication

The commercial high purity α-Al_2O_3 (>99.99%, $D_{50} \approx 0.38$ μm), Y_2O_3 (>99.99%, $D_{50} \approx 3.35$ μm), and Tm_2O_3 (>99.99%, $D_{50} \approx 2.0$ μm) were used as starting materials. To fabricate the specimens, those starting powders were weighed according to the different Tm contents in the resultant YAG ceramics (from 0.18 at.% to 3.0 at.%). After the Al_2O_3, Y_2O_3, and Tm_2O_3 powders had been mixed with different mass ratios of tetraethyl orthosilicate (TEOS) according to the different Tm contents as a sintering aid (from 0.5 mass% to 1.0 mass%), the mixture was milled for 12 h with high-purity Al_2O_3 balls. After dried and sieved through 200-

* Corresponding author. Tel.: +86 21 52412820; fax: +86 21 52413903.
E-mail address: ybpan@mail.sic.ac.cn (Y.B. Pan).

0272-8842/$36.00.
doi:10.1016/j.ceramint.2010.11.023

mesh screen, the powders were calcined at 400–800 °C for 2 h to remove the organic component and then dry-pressed at 3 T to form a disk with a diameter of 25 mm and follow-up isostatically cold-pressed at 250 MPa. The powder compacts were vacuum-sintered at 1780 °C for 20 h under 10^{-3} Pa, then annealed at 1450 °C for 20 h under atmosphere.

2.2. Characterizations

Micrographs of the starting powders were observed by a field emission scanning electron microscopy (FESEM, Model JSM-6700, JEOL, Japan). Phase compositions of the obtained samples were identified by X-ray diffraction (XRD, Model D/max2200PC, Rigaku, Japan). The samples mirror-polished on both surfaces were used to measure optical transmittance (Model U-2800 Spectrophotometer, Hitachi, Tokyo, Japan).

The oscillation threshold and the re-absorption loss increase with the Tm^{3+}-doping concentration, which will induce the decreasing of the slope efficiency. Therefore, it is quite important to choose the proper doping concentration of Tm^{3+}. In this work, we employed 6 at.% Tm:YAG sample to realize the laser operation (carried out by the Institute of Physics, Chinese Academy of Sciences).

The microstructures of the mirror-polished surface and grain boundary of 6 at.% Tm:YAG sample were observed by electron probe micro-analyzer (EPMA, Model JXA-8100, JEOL, Tokyo, Japan) and field emission transmission electron microscopy (FETEM, Model EM 2100, JEOL, Tokyo, Japan), respectively.

3. Results and discussion

Powders within the nanometric range are generally selected for the reactive sintering process of these materials with the purpose of improving the density and limiting the grain growth [10–13]. However, the handling and contamination control of nanometric powders are often difficult and the reliability of the process is poor [10,14]. Micrometric powders, on the other hand, if properly shaped may equally promote homogeneous particle coordination and at the same time result in the formation of fine grained microstructures [15].

The FESEM micrographs of the micrometric starting powders used in this work are shown in Fig. 1. It can be seen that the primary particle sizes of Y_2O_3, α-Al_2O_3 and Tm_2O_3 powders are 3.35, 0.38 and 2.0 μm, respectively. After ball milling, the large particles of Y_2O_3, Tm_2O_3 and the fine particles of α-Al_2O_3 have been homogeneously mixed.

The XRD patterns obtained for $(Y_{3-x}Tm_x)Al_5O_{12}$ ($x = 0$, 0.18, 0.9, 1.5, 3) samples (Fig. 2) are well indexable under Ia–3d lattice symmetry consistent with the standard JCPDF files [# 79-1892 for $Y_3Al_5O_{12}$ (YAG) and # 17-0734 for $Tm_3Al_5O_{12}$ (TAG)]. Fig. 2 shows that the samples with different concentration of thulium ions doped into YAG are still in pure phases and the host structure is changed into TAG as the amount of thulium ion increases. Also, the peaks of the XRD patterns slightly move right with the increase of concentration of thulium ions being the Tm^{3+} radius (86.9 pm) a little smaller than that of Y^{3+} (90 pm).

Fig. 3 is the in-line transmittance spectra and photos of four samples with Tm content of 6%, 30%, 50%, 100%, respectively. It can be seen that Tm:YAG ceramics with excellent optical properties have been obtained through the vacuum-sintering preparation. Along with the increasing Tm content, the specimens look greener due to the light absorption of Tm^{3+} at the visible band. Moreover, all the main absorption bands of Tm^{3+} are distinctively strengthened with more Tm added, and that means Tm^{3+} ions take the place of Y^{3+} ions

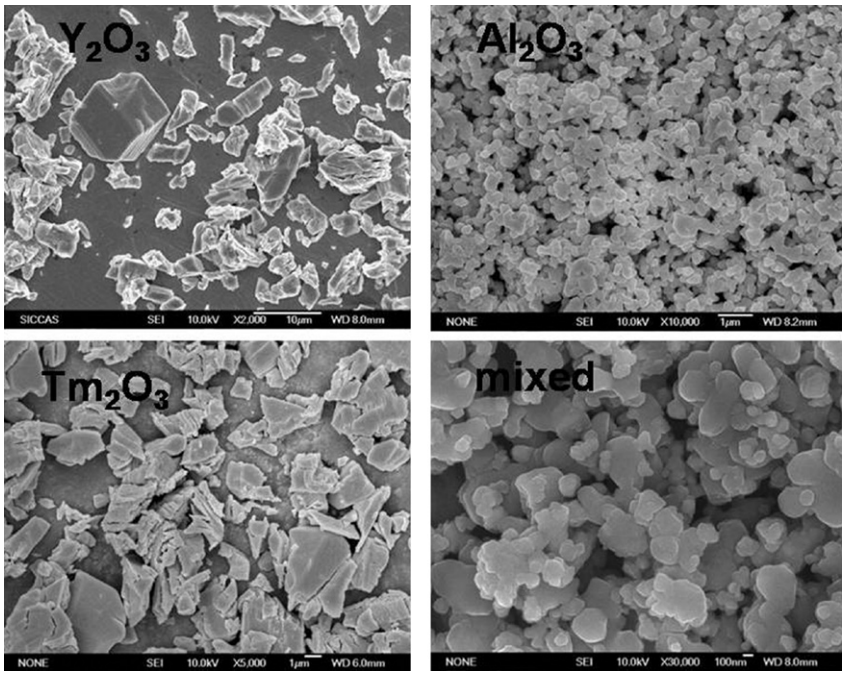

Fig. 1. The FESEM micrographs of the micrometric starting powders.

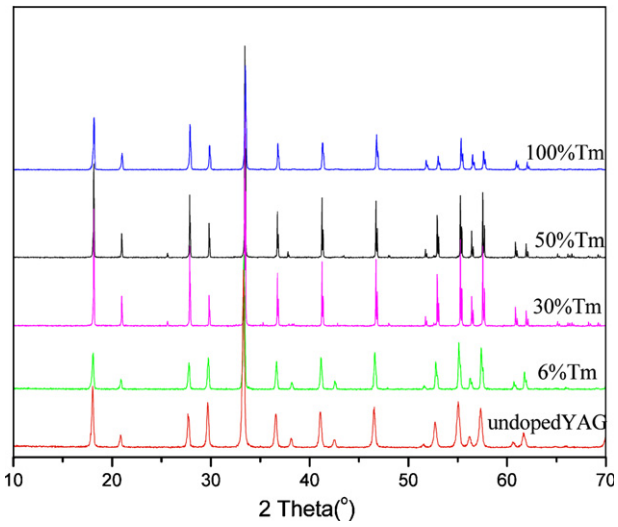

Fig. 2. The XRD patterns of $(Y_{3-x}Tm_x)Al_5O_{12}$ ($x = 0$, 0.18, 0.9, 1.5, 3) samples.

successfully owing to their similar chemical properties and ionic radii. And the absorption bands centered at 262 nm, 357 nm, 460 nm, 681 nm, 785 nm, 1172 nm, and 1622 nm correspond to energy level $^3P_2$, $^1D_2$, $^1G_4$, $^3F_3$–$^3F_2$, $^3H_4$, $^3H_5$, and $^3F_4$, respectively.

The 6 at.% Tm:YAG ceramic sample was thermal-etched after mirror polishing in order to observe the microstructure of the grains and the grain boundaries by EPMA. Fig. 4(a) shows that the average grain size is about 15 μm and there are no pores and impurities in or between the grains. Fig. 4(b) shows the EDS line scan analysis of Tm:YAG ceramic obtained by EPMA. The Al, Y, Tm and Si contents remain steady across the grain boundary, indicative of an even distribution of the elements.

The high-resolution TEM (HRTEM) micrograph of the grain boundary in the 6 at.% Tm:YAG ceramics is shown in Fig. 5. The grain boundary is clean and narrow with a width of about 1 nm, so the optical scattering caused by boundaries will be insignificant, which also has been proved in previous papers [16,17].

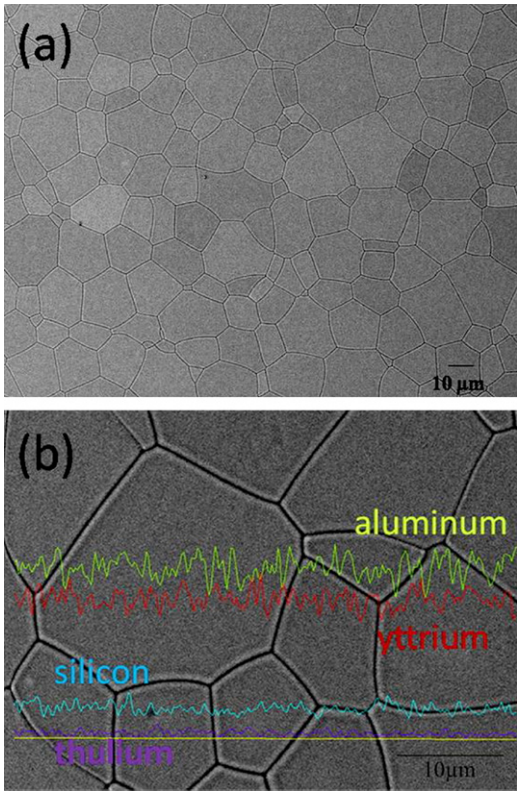

Fig. 4. The EPMA micrograph and the EDS line scan analysis of the mirror-polished and thermal-etched surface of the 6 at.% Tm:YAG ceramic.

The 6 at.% Tm:YAG ceramic sample (5 mm × 5 mm × 3.5 mm) was end-pumped by a Ti:sapphire laser with an emission wavelength of 785 nm. Fig. 6(a) shows the laser output power versus the absorbed pump power for the 6 at.% Tm:YAG ceramic. With maximum absorbed pump power of 2.1 W, laser output power of 725 mW has been obtained using the output coupler (OC) with 3% transmission at 2012 nm. The slope efficiency and optic–optic transformation efficiency of Tm:YAG ceramic are 36.2% and 19.9%, respectively. Fig. 6(b) displays the laser spectrum of the

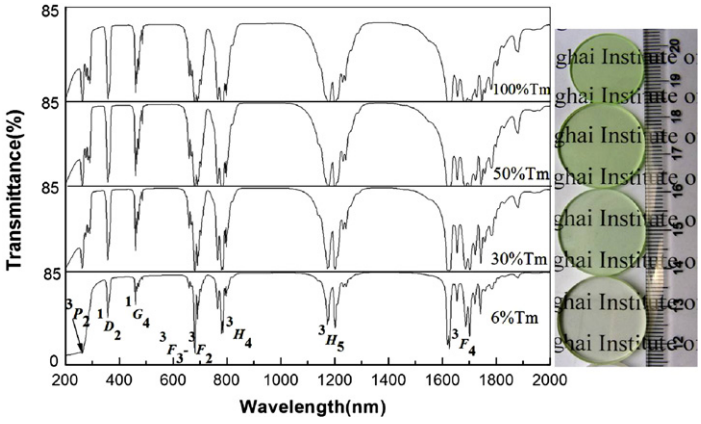

Fig. 3. The in-line transmittance spectra and photos of four samples with Tm content of 6%, 30%, 50%, 100%.

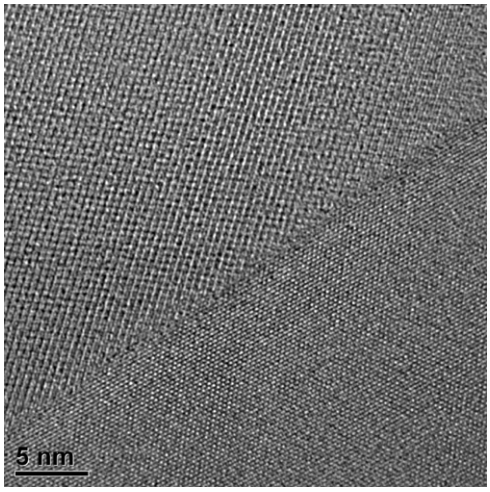

Fig. 5. The high-resolution TEM (HRTEM) micrograph of the grain boundary.

6 at.% Tm:YAG ceramic. The central wavelength is 2012 nm with the spectral linewidth of 3 nm. The results of the laser experiment show that the quality of such kind of ceramic is good enough to be used as a highly efficient laser material and is a very promising substitute for Tm:YAG crystal in the foreseeable future.

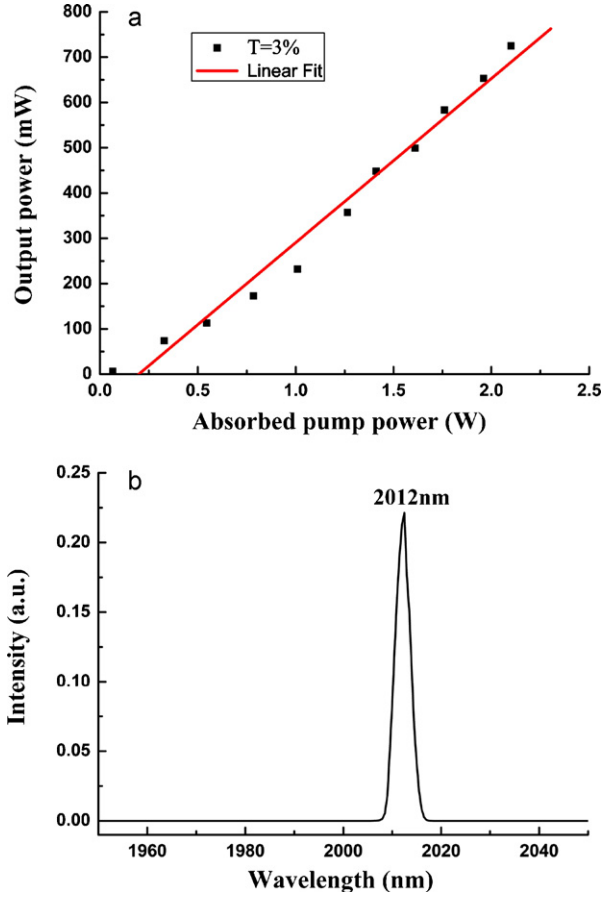

Fig. 6. The laser output power versus the absorbed pump power (a) and the laser spectrum (b) for the 6 at.% Tm:YAG ceramic.

4. Conclusions

Phase-pure, nanograined (15 μm) and highly transparent $(Y_{3-x}Tm_x)Al_5O_{12}$ ($x = 0$, 0.18, 0.9, 1.5, 3) ceramics were successfully fabricated by solid-state reaction and vacuum sintering. The maximum output power of 725 mW for the $Y_{2.82}Tm_{0.18}Al_5O_{12}$ (6 at.% Tm:YAG) ceramic slab (5 mm × 5 mm × 3.5 mm) end-pumped by a Ti:sapphire laser at 785 nm was obtained with a slope efficiency of 36.2% and optical-to-optical efficiency of 19.9% at 2012 nm. This supports the view that Tm:YAG ceramic would be a very promising highly efficient laser material in the foreseeable future.

Acknowledgments

The authors acknowledge Dr. Yu-Wan Zou and Prof. Zhi-Yi Wei for the laser experiment. This work was supported by the 863 project (No. AA03Z523), NSFC (No. 50990300) and the Major Basic Research Programs of Shanghai (No. 07DJ14001).

References

[1] G. Rustad, K. Stenersen, Low threshold laser-diode side-pumped Tm:YAG and Tm:Ho:YAG lasers, IEEE J. Sel. Top. Quantum Electron. 3 (1) (1997) 82–89.
[2] A. Ikesue, T. Kinoshita, K. Kamata, K. Yoshida, Fabrication and optical properties of high-performance polycrystalline Nd:YAG ceramics for solid-state laser, J. Am. Ceram. Soc. 78 (1995) 1033–1040.
[3] A. Ikesue, K. Kamata, K. Yoshida, Synthesis of transparent Nd-doped HfO_2–Y_2O_3 ceramics using HIP, J. Am. Ceram. Soc. 79 (1996) 359–364.
[4] Y. Sato, I. Shoji, T. Taira, A. Ikesue, The spectroscopic properties and laser characteristics of polycrystalline Nd:$Y_3Sc_xAl_{(5-x)}O_{12}$ laser media, OSA-TOPS 83 (2003) 444.
[5] J. Lu, J. Lv, T. Murai, K. Takaichi, T. Uematsu, K. Ueda, H. Yagi, T. Yanagitani, A. Kaminskii, Nd^{3+}:Y_2O_3 ceramic laser, Jpn. J. Appl. Phys. 40 (2001) 1277–1279.
[6] J. Lu, J.F. Bisson, K. Takaichi, T. Uematsu, A. Shirakawa, M. Musha, K. Ueda, H. Yagi, T. Yanagitani, A. Kaminskii, Yb^{3+}:Sc_2O_3 ceramic laser, Appl. Phys. Lett. 83 (6) (2003) 1101–1103.
[7] J. Lu, K. Takaichi, T. Uematsu, A. Shirakawa, M. Musha, K. Ueda, H. Yagi, T. Yanagitani, A. Kaminskii, Yb^{3+}:Y_2O_3 ceramics—a novel solid-state laser materials, Jpn. J. Appl. Phys. 41 (2002) 1373–1375.
[8] J. Lu, K. Takaichi, T. Uematsu, A. Shirakawa, M. Musha, K. Ueda, H. Yagi, T. Yanagitani, A. Kaminskii, Promising ceramic laser material: highly transparent Nd^{3+}:Lu_2O_3 ceramic, Appl. Phys. Lett. 81 (2002) 4324.
[9] J. Saikawa, Y. Sato, T. Taira, A. Ikesue, Absorption, emission spectrum properties, and efficient laser performances of Yb:$Y_3ScAl_4O_{12}$ ceramics, Appl. Phys. Lett. 85 (2004) 1898–1900.
[10] A. Krell, T. Hutzler, J. Klimke, Transparent ceramics for structural applications. Part 1. Physics of light transmission and technological consequences, Ceram. Forum Int. 84 (4) (2007) 41–50.
[11] Y. Rabinovitch, D. Tétard, M.D. Faucher, M. Pham-Thi, Transparent polycrystalline neodymium doped YAG: synthesis parameters laser efficiency, Opt. Mater. 24 (1–2) (2003) 345–351.
[12] N. Matsushita, N. Tsuchiya, K. Natatsuka, T. Yanagitani, Precipitation and calcination process for yttrium aluminum garnet precursors synthesized by the urea method, J. Am. Ceram. Soc. 82 (8) (1999) 1977–1984.
[13] T. Feng, J. Shi, D. Jiang, Preparation and optical properties of transparent Eu^{3+}:$Y3Al_{5(1-x)}Sc_{5x}O_{12}$ ceramics, J. Am. Ceram. Soc. 89 (5) (2006) 1590–1593.

[14] A.L. Costa, L. Esposito, V. Medri, A. Bellosi, Synthesis of Nd-YAG material by citrate nitrate sol–gel combustion route, Adv. Eng. Mater. 9 (4) (2007) 307–312.

[15] L. Esposito, A. Piancastelli, Role of powder properties and shaping techniques on the formation of pore-free YAG materials, J. Eur. Ceram. Soc. 29 (2) (2007) 317–322.

[16] A. Ikesue, K. Kamata, K. Yoshida, Synthesis of Nd^{3+}, Cr^{3+}-codoped YAG ceramics for high-efficiency solid-state lasers, J. Am. Ceram. Soc. 78 (1995) 2545–2547.

[17] A. Ikesue, K. Kamata, T. Yamamoto, I. Yamaga, Optical scattering centers in polycrystalline Nd:YAG laser, J. Am. Ceram. Soc. 80 (6) (1997) 1517–1522.